CRACK TIP FIELD AND *J*-INTEGRAL WITH STRAIN GRADIENT EFFECT*

XIA Song (夏 嵩)†   WANG Tzuchiang (王自强)   CHEN Shaohua (陈少华)

(*LNM, Institute of Mechanics, Chinese Academy of Sciences, Beijing 100080, China*)

ABSTRACT: The mode I plane strain crack tip field with strain gradient effects is presented in this paper based on a simplified strain gradient theory within the framework proposed by Acharya and Bassani. The theory retains the essential structure of the incremental version of the conventional J_2 deformation theory. No higher-order stress is introduced and no extra boundary value conditions beyond the conventional ones are required. The strain gradient effects are considered in the constitutive relation only through the instantaneous tangent modulus. The strain gradient measures are included into the tangent modulus as internal parameters. Therefore the boundary value problem is the same as that in the conventional theory. Two typical crack problems are studied: (a) the crack tip field under the small scale yielding condition induced by a linear elastic mode-I K-field and (b) the complete field for a compact tension specimen. The calculated results clearly show that the stress level near the crack tip with strain gradient effects is considerable higher than that in the classical theory. The singularity of the strain field near the crack tip is nearly equal to the square-root singularity and the singularity of the stress field is slightly greater than it. Consequently, the J-integral is no longer path independent and increases monotonically as the radius of the calculated circular contour decreases.

KEY WORDS: strain gradient, FEM, crack tip field, J-integral

1 INTRODUCTION

Elssner et al.[1] estimated the stress level near the tip of an interfacial crack between a niobium single crystal and a sapphire single crystal in a series of experiments. It is about 10 times the tensile yield stress. Hutchinson[2] pointed out, however, that according to the classical theory of plasticity, that stress level should not have been more than 4~5 times the yield stress. In addition, Elssner et al.[1] observed that the interface between those two materials remained atomistically sharp, i.e., the crack tip was not blunted even though there were a large number of dislocations in niobium. It is an evident contradiction between the experimental results and the classical theory of plasticity.

The problem may be solved through strain gradient plasticity theories. With the strain gradient mea-sures added into the theory of plasticity, the theoretical stress level may become somewhat higher than the classical one. Therefore, there are many studies to apply the theories of strain gradient plasticity into fracture analyses.

For CS (couple-stress) theory of strain gradient plasticity [3,4], both the asymptotic analysis [5~8] and FEM calculation [7,9] found that the stress level estimated near a crack tip is essentially the same as that in the classical plasticity. It is because that no effect of stretch gradient is considered in CS theory.

Wei and Hutchinson[10], Chen et al.[11] and Shi et al.[12] have used a general phenomenological strain gradient plasticity theory[13] to study the crack tip field. The elevation of stress level is indeed observed in their analyses. But as a mode-I crack tip is approached, the traction is found to switch to compression. It is therefore concluded by Chen et al.[11] that

the asymptotic crack tip field in this theory has no domain of physical validity.

Based on MSG (mechanism-based strain gradient) plasticity theory [14,15], Shi et al.[16] investigated the asymptotic crack tip field and concluded that this field in MSG theory is inseparable. Jiang et al.[17] presented the crack tip field with FEM of MSG theory. They observed the stress elevation and found that the stress singularity exceeded or was equal to the square-root singularity.

In all work mentioned above, third-order stresses or couple stresses are considered, which made the analysis quite laborious. Retaining the essential structure of the conventional plasticity, Acharya and Bassani[18] concluded that it is thermodynamically possible to formulate a flow theory with strain gradient measures incorporated into the instantaneous hardening functions while preserving the linear relationship between rate quantities. However, they didn't give a systematic way of constructing the tangent modulus to validate this framework. Following their thought, Chen and Wang[19] established a new hardening law based on the incremental version of classical J_2 deformation theory. The effective strain gradient is only a parameter to influence the tangent modulus in that hardening law. Chen and Wang[20,21] established a new version of the phenomenological strain gradient theory for crystalline solids and stretch gradients are introduced in a similar way as by Chen and Wang[19]. Based on the new theory, both the asymptotic fields [21,22] and the full field solution[23] are studied.

The present work is motivated by Chen and Wang[19]. A simplified strain gradient theory based on the incremental version of conventional J_2 deformation theory is presented here, in which the strain gradient measures are only parameters to influence the tangent modulus. In Section 2, the new constitutive relation is outlined. The FEM formulation is introduced in Section 3 and the calculated results are discussed in Section 4.

2 NONLINEAR CONSTITUTIVE RELATION WITH STRAIN GRADIENTS

The simplified strain gradient theory used here is within the framework proposed by Acharya and Bassani[18]. The essential structure of the classical deformation theory is preserved and no extra boundary conditions beyond the conventional ones are required in the simplified strain gradient theory. No higher-order stress or higher-order strain rates are introduced either.

The work done on the solid per unit volume is equal to the increment of the strain energy

$$\delta w = s_{ij}\delta e_{ij} + \frac{\sigma_{kk}}{3}\delta\varepsilon_{ll} \qquad (2.1)$$

where σ_{ij} is the stress, ε_{ij} is the strain, s_{ij} is the deviatoric stress and e_{ij} is the deviatoric strain. The nonlinear stress-strain relation is

$$\sigma_{ij} = \frac{2\sigma_e}{3\varepsilon_e}e_{ij} + K\delta_{ij}\varepsilon_{kk} \qquad (2.2)$$

where δ_{ij} is the Kronecker delta and

$$K = \frac{E}{3(1-2\nu)} \qquad (2.3)$$

where E is Young's modulus and ν is Poisson's ratio.

The incremental version of Eq.(2.3) is

$$\dot{\sigma}_{ij} = \frac{2\sigma_e}{3\varepsilon_e}\dot{e}_{ij} + \frac{2\dot{\sigma}_e}{3\varepsilon_e}e_{ij} - \frac{2\sigma_e}{3\varepsilon_e^2}\dot{\varepsilon}_e e_{ij} + K\delta_{ij}\dot{\varepsilon}_{kk} \qquad (2.4)$$

where $\sigma_e = (3s_{ij}s_{ij}/2)^{1/2}$ is the effective stress and $\varepsilon_e = (2e_{ij}e_{ij}/3)^{1/2}$ is the effective strain.

In the classical deformation theory, the hardening relation is

$$\sigma_e = \sigma_0 A(\varepsilon_e) \qquad (2.5)$$

where σ_0 is the yielding stress and $A(\varepsilon_e)$ is the work hardening function. Thus

$$\dot{\sigma}_e = \sigma_0 A'(\varepsilon_e)\dot{\varepsilon}_e \qquad (2.6)$$

where $A'(\varepsilon_e)$ is the tangent hardening modulus in the incremental version of the conventional J_2 deformation theory.

According to the Taylor's hardening relation, the flow strength σ is related to the dislocation density ρ as

$$\sigma = CGb\sqrt{\rho} \qquad (2.7)$$

where C is a constant coefficient, G is the shear modulus and b is the magnitude of Burger's vector $\boldsymbol{b}$.

As pointed out by Ashby [24], the dislocations are stored as two types: the statistically stored dislocations and the geometrically necessary dislocations. Then the flow strength is

$$\sigma = CGb\sqrt{\rho_S + \rho_G} = CGb\sqrt{\rho_S}\sqrt{1 + \frac{\rho_G}{\rho_S}} \qquad (2.8)$$

where ρ_S is the statistically stored dislocation density and ρ_G is the geometrically necessary dislocation density.

The density ρ_S has been characterized as a function of the effective strain measure ε_e by numerous

investigators, where a strain gradient measure is accommodated by geometrically necessary dislocations. Hence, Gao et al.[4] proposed that the flow strength in the presence of strain gradients can be expressed as

$$\sigma = \sigma_0 A(\varepsilon_e)\sqrt{1 + \frac{l\eta}{A^2(\varepsilon_e)}} \qquad (2.9)$$

where l is a material length scale and η is a strain gradient measure.

According to Fleck and Hutchinson [13], the expression of $l\eta$ is

$$l\eta = \sqrt{l_1^2\eta_1^2 + l_{CS}^2\chi_e^2} \qquad (2.10)$$

where $l = l_{CS}$, l_1 and l_{CS} are two constant material length scales; $\eta_1 = \sqrt{\eta_{ijk}^{(1)}\eta_{ijk}^{(1)}}$, $\eta_{ijk}^{(1)}$ is one of the three mutually orthogonal third-order deviatoric strain gradient tensors defined by Smyshlyaev and Fleck[25].

Since the calculation of η_1 seems somewhat complex, a simplified strain gradient measure is proposed in the present paper

$$l\eta = l_1\eta_e + l_{CS}\chi_e \qquad (2.11)$$

and

$$\eta_e = \sqrt{\varepsilon_{e,k}\varepsilon_{e,k}} \qquad \chi_e = \sqrt{\frac{2}{3}\chi_{ij}\chi_{ij}} \qquad (2.12)$$

where χ_{ij} is the curvature tensor. The gradient of the effective strain η_e was first proposed by Aifantis[26] and it is accommodated to the stretch gradients while the effective curvature χ_e represents the rotation gradients. The expression (2.11) is essentially the same as that of Eq.(2.10) but more simple from the point of view of computation.

In the present theory, Eqs.(2.1)~(2.4) will be retained. Only the tangent modulus in Eq.(2.6) will be multiplied by a coefficient R. Following the proposal by Chen and Wang [21,23], this coefficient can be expressed as

$$R = \sqrt{1 + \frac{l_1\eta_e + l_{CS}\chi_e}{\varepsilon_e}} \qquad (2.13)$$

Then Eq.(2.6) can be rewritten as

$$\dot{\sigma}_e = \sigma_0 A'(\varepsilon_e)R\dot{\varepsilon}_e \qquad (2.14)$$

Substitute Eq.(2.14) into Eq.(2.4), we get

$$\dot{\sigma}_{ij} = \frac{2\sigma_e}{3\varepsilon_e}\dot{e}_{ij} + \frac{2\sigma_0 A'(\varepsilon_e)R}{3\varepsilon_e}\dot{\varepsilon}_e e_{ij} -$$

$$\frac{2\sigma_e}{3\varepsilon_e^2}\dot{\varepsilon}_e e_{ij} + K\delta_{ij}\dot{\varepsilon}_{kk} \qquad (2.15)$$

Since

$$\dot{\varepsilon}_e = \frac{2e_{kl}}{3\varepsilon_e}\dot{e}_{kl} = \frac{2e_{kl}}{3\varepsilon_e}\dot{\varepsilon}_{kl}$$

$$\dot{\varepsilon}_{kk} = \delta_{kl}\dot{\varepsilon}_{kl}$$

$$\dot{e}_{ij} = \dot{\varepsilon}_{ij} - \frac{1}{3}\delta_{ij}\dot{\varepsilon}_{kk} = \delta_{ik}\delta_{jl}\dot{\varepsilon}_{kl} - \frac{1}{3}\delta_{ij}\delta_{kl}\dot{\varepsilon}_{kl}$$

Eq.(2.15) can be rewritten as

$$\dot{\sigma}_{ij} = \left(B\delta_{ik}\delta_{jl} + \frac{3K - B}{3}\delta_{ij}\delta_{kl} + Ce_{ij}e_{kl}\right)\dot{\varepsilon}_{kl} \quad (2.16)$$

where

$$B = \frac{2\sigma_e}{3\varepsilon_e}$$
$$\qquad\qquad\qquad\qquad (2.17)$$
$$C = \frac{2}{3\varepsilon_e^2}\left(\frac{2}{3}\sigma_0 A'(\varepsilon_e)R - B\right)$$

If the exponent hardening relation is used, we have

$$A(\varepsilon_e) = \begin{cases} 2\mu & \sigma_e < \sigma_0 \\ \left(\dfrac{\varepsilon_e}{\varepsilon_0}\right)^n & \sigma_e \geq \sigma_0 \end{cases} \qquad (2.18)$$

and

$$A'(\varepsilon_e) = \begin{cases} 0 & \sigma_e < \sigma_0 \\ \dfrac{n\varepsilon_e^{n-1}}{\varepsilon_0^n} & \sigma_e \geq \sigma_0 \end{cases} \qquad (2.19)$$

where n is the hardening exponent, ε_0 is the reference strain and

$$\varepsilon_0 = \frac{2(1 + \nu)\sigma_0}{3E} = \frac{\sigma_0}{3\mu} \qquad (2.20)$$

Let

$$D_{ijkl}^{(1)} = \delta_{ik}\delta_{jl}$$

$$D_{ijkl}^{(2)} = \delta_{ij}\delta_{kl} \qquad (2.21)$$

$$D_{ijkl}^{(3)} = e_{ij}e_{kl}$$

and then

$$\dot{\sigma}_{ij} = \begin{cases} \left(2\mu D_{ijkl}^{(1)} + \dfrac{3K - 2\mu}{3}D_{ijkl}^{(2)}\right)\dot{\varepsilon}_{kl} \\ \qquad \sigma_e < \sigma_0 \\ \left(BD_{ijkl}^{(1)} + \dfrac{3K - B}{3}D_{ijkl}^{(2)} + CD_{ijkl}^{(3)}\right)\dot{\varepsilon}_{kl} \\ \qquad \sigma_e \geq \sigma_0 \end{cases}$$
$$(2.22)$$

where $\mu = E/[2(1 + \nu)]$ is the shear modulus, E is Young's modulus and ν is Poisson's ratio.

3 FEM SIMULATION

For a solid in the present strain gradient theory, the principle of virtual work is

$$\int_V \left(s_{ij}\delta e_{ij} + \frac{\sigma_{kk}}{3}\delta\varepsilon_{ll}\right)\mathrm{d}V - \int_{S_\sigma} t_i^0\delta u_i\mathrm{d}S = 0 \quad (3.1)$$

where t_i^0 is the prescribed traction on the boundary and S_σ is the surface portion of the solid where tractions are prescribed.

For the FEM formulation of a plane-strain problem, suppose that the z-axis is identical with the crack front, the y-axis perpendicular to the crack surface and the positive half of the x-axis lying ahead of the crack (as shown in Fig.1). Equation (2.22) can be rewritten as

$$\dot{\sigma} = \begin{cases} \left(2\mu D^{(1)} + \dfrac{K-2\mu}{3}D^{(2)}\right)\dot{\varepsilon} \\ \qquad\qquad \sigma_e < \sigma_0 \\ \left(B D^{(1)} + \dfrac{K-B}{3}D^{(2)} + CD^{(3)}\right)\dot{\varepsilon} \\ \qquad\qquad \sigma_e \geq \sigma_0 \end{cases} \quad (3.2)$$

where

$$\dot{\sigma} = \begin{pmatrix} \dot{\sigma}_{xx} & \dot{\sigma}_{yy} & \dot{\tau}_{xy} \end{pmatrix}^{\mathrm{T}} \quad (3.3)$$

$$\dot{\varepsilon} = \begin{pmatrix} \dot{\varepsilon}_{xx} & \dot{\varepsilon}_{yy} & \dot{\gamma}_{xy} \end{pmatrix}^{\mathrm{T}} \quad (3.4)$$

$$D^{(1)} = \begin{bmatrix} 1 & 0 & 0 \\ 0 & 1 & 0 \\ 0 & 0 & 1/2 \end{bmatrix} \quad (3.5)$$

$$D^{(2)} = \begin{bmatrix} 1 & 1 & 0 \\ 1 & 1 & 0 \\ 0 & 0 & 0 \end{bmatrix} \quad (3.6)$$

$$D^{(3)} = \begin{bmatrix} e_{xx}^2 & e_{xx}e_{yy} & e_{xx}e_{xy} \\ e_{yy}e_{xx} & e_{yy}^2 & e_{yy}e_{xy} \\ e_{xy}e_{xx} & e_{xy}e_{yy} & e_{xy}^2 \end{bmatrix} \quad (3.7)$$

and

$$\dot{\sigma}_{zz} = \begin{cases} \dfrac{3K-2\mu}{3}\left(\dot{\varepsilon}_{xx} + \dot{\varepsilon}_{yy}\right) & \sigma_e < \sigma_0 \\ \dfrac{3K-B}{3}\left(\dot{\varepsilon}_{xx} + \dot{\varepsilon}_{yy}\right) + Ce_{zz}\cdot \\ \left(e_{xx}\dot{\varepsilon}_{xx} + e_{yy}\dot{\varepsilon}_{yy} + e_{xy}\dot{\gamma}_{xy}\right) & \sigma_e \geq \sigma_0 \end{cases} \quad (3.8)$$

The non-vanishing displacement components in a plane-strain problem are

$$u_x = u_x(x,y) \qquad u_y = u_y(x,y) \qquad (3.9)$$

The J-integral of a plane-strain mode-I crack is

$$J_1 = \int_\Gamma (wn_1 - n_\alpha\sigma_{\alpha\beta}u_{\beta,1})\mathrm{d}\Gamma \qquad (3.10)$$

where Γ is a contour starting from the lower surface of the crack and ending at the upper one; n_α is the normal of Γ; α, $\beta = 1,2$; w is the strain energy density and

$$w = \int s_{ij}\mathrm{d}e_{ij} + \int \frac{\sigma_{kk}}{3}\mathrm{d}\varepsilon_{ll} \qquad (3.11)$$

Two typical crack problems are studied here. First the crack tip field under the small scale yielding condition is investigated.

The calculated domain is a circular domain centered at the crack tip as shown in Fig.1(a). The radius of the circular domain is a. The classical mode-I K-field is imposed on the outer boundary of this domain (as shown in Fig.1(a)). The crack surface is supposed to be traction-free and the elastic stress intensity factor, K_{I}, of the remotely applied field increases monotonically.
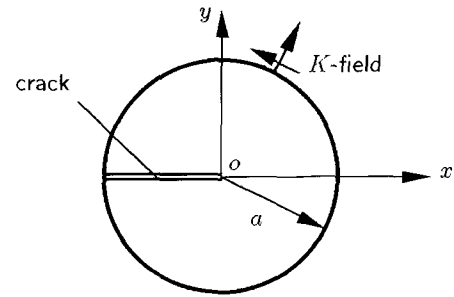
(a) The crack tip field under the small scale yielding condition induced by a linear elastic mode-I K-field
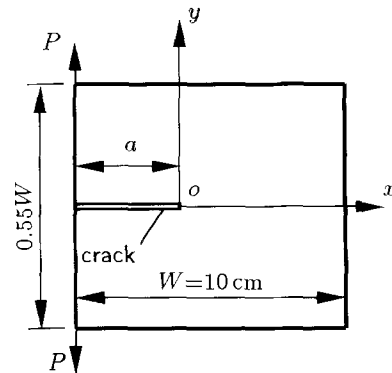
(b) The complete field for a compact tension specimen

Fig.1 The calculated domain

Second the complete field of a compact tension specimen as shown in Fig.1(b) is studied. The specimen width is W and crack length is a. The value of a is usually $0.45 \sim 0.55W$ in a compact tension specimen. Here it is taken as $0.5W$. The applied load is P.

An eight-node isoparametric element is chosen and each node has two degrees of freedom. For the first problem shown in Fig.1(a) (Problem A), the ratio of l_1/a is about 10^{-7} to 10^{-3} and the size of the

smallest elements is less than $10^{-3}l_1$. For the second problem shown in Fig.1(b) (Problem B), the value of l_1/W is about 10^{-6} to 10^{-5}. The ratio of the length to the width of the elements is made to be approximately equal to a value of unity. In both problems, only the upper half of the domain is calculated due to the symmetric condition. The half domain is divided circumferentially into 12 portions and radially into N_r portions, respectively. In order to investigate the influence of the mesh, the value of N_r is taken as 30, 50, 100 and 200, respectively for Problem A. The calculated results are shown in Fig.2. It is evident that when $N_r = 30$, the calculated results deviated from the other results obviously. Since the results for $N_r = 50$, 100 and 200 are almost identical, we will take $N_r = 50$ for Problem A and $N_r = 80$ for Problem B in the following calculations.
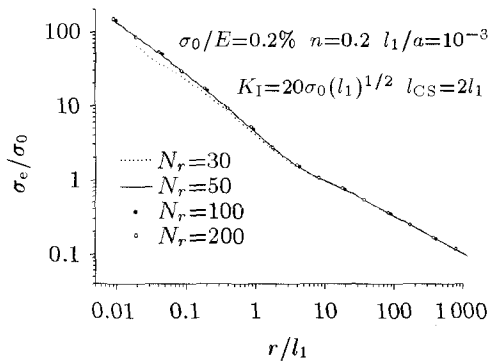

Fig.2 Calculated effective stress σ_e with different meshes

4 CALCULATED RESULTS

In order to verify the reliability of the present program, we first investigate the case of the classical deformation theory. With $l_1 = 0$, our calculation is compared with the result of Chen and Wang[23] for Problem A. Both results are plotted in Fig.3. The parameters are the same as those by Chen and Wang [23]: $\sigma_0/E = 0.2\%$, $\nu = 0.3$, $n = 0.2$, $K_I = 20\sigma_0(l_1)^{1/2}$. The two results are almost identical, which means that our program is reliable.

The calculated results for Problem A are shown in Figs.4~11.

The effect of the material length scale l_1 on the effective stress σ_e near the crack tip is shown in Fig.4. The material parameters are: $\sigma_0/E = 0.2\%$, $\nu = 0.3$, $n = 0.2$, $K_I = \sigma_0(a)^{1/2}$ and $l_{CS} = 2l_1$. One can see from Fig.4 that there is a domain dominated by the strain gradient near the crack tip. The singularities of the near-tip stress field are almost the same for diff-
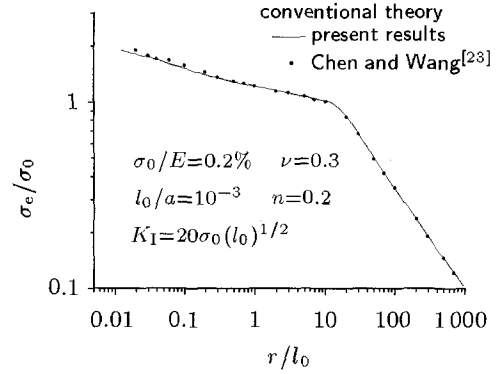

Fig.3 Comparison with Chen and Wang[23], without strain gradient effects, l_0 is a reference length
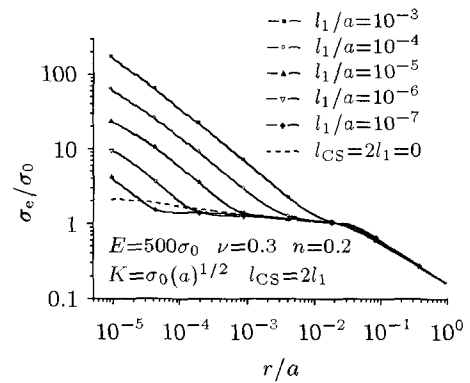

Fig.4 Normalized effective stress σ_e/σ_0 versus normalized distance r/a with various values of l_1/a for both the strain gradient theory and classical theory
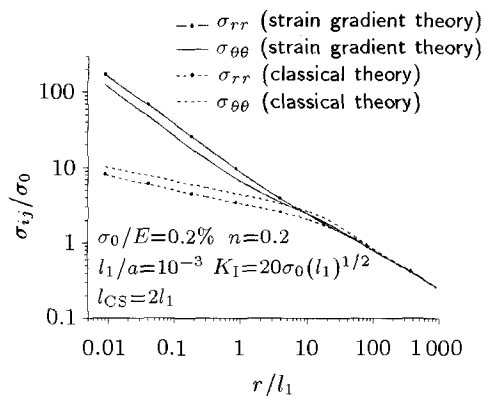

Fig.5 Normalized stress components σ_{rr}/σ_0 and $\sigma_{\theta\theta}/\sigma_0$ versus normalized distance r/l_1 for both the strain gradient theory and classical theory
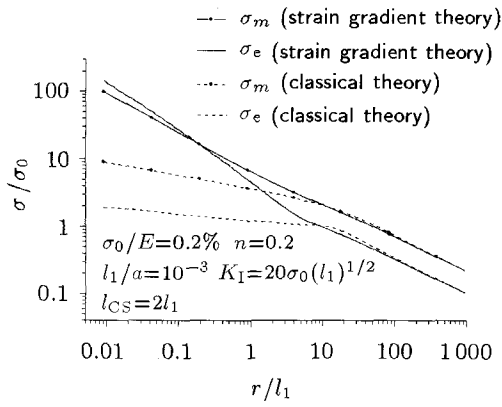
Fig.6 Normalized mean stress σ_m/σ_0 and effective stress σ_e/σ_0 versus normalized distance r/l_1 for both the strain gradient theory and classical plasticity theory
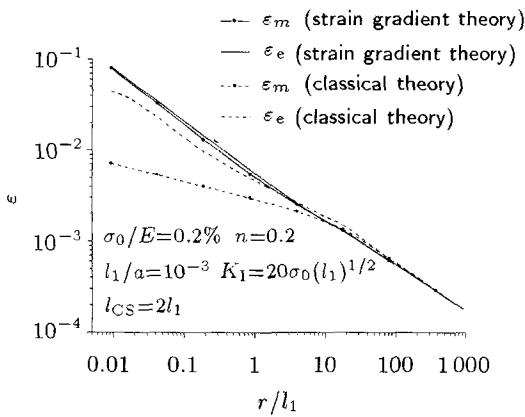

Fig.7 Hydrostatic strain ε_m and effective strain ε_e versus normalized distance r/l_1 for both the strain gradient theory and classical plasticity theory
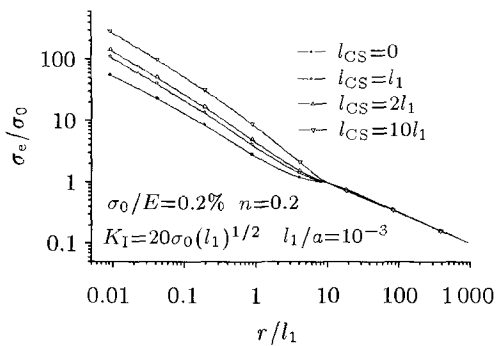

Fig.8 Normalized effective stress σ_e/σ_0 versus normalized distance r/l_1 with various values of l_{CS}/l_1
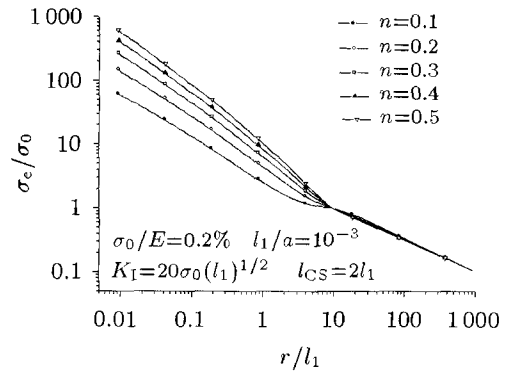

Fig.9 Normalized effective stress σ_e/σ_0 versus normalized distance r/l_1 with various values of hardening exponent n
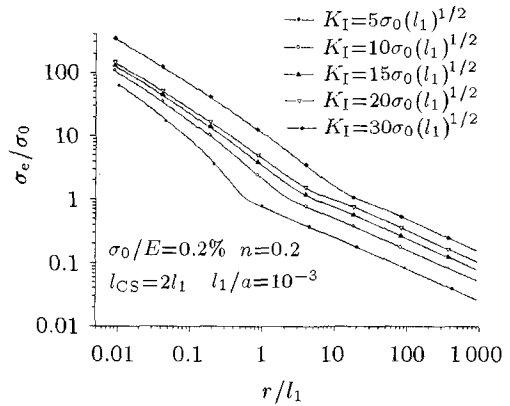

Fig.10 Normalized effective stress σ_e/σ_0 versus normalized distance r/l_1 with various values of stress intensity factor K_I
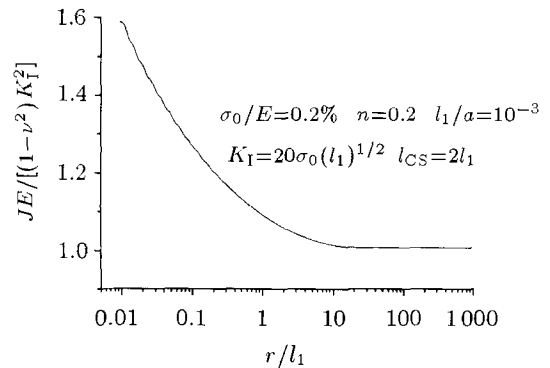

Fig.11 Normalized J-integral $JE/[(1-\nu^2)K_I^2]$ versus normalized distance r/l_1

erent material length scales l_1. Outside of the strain-gradient-dominated domain, it is observed that all the results are almost identical where the strain gradient effects can be neglected. Away from the crack tip, there are an HRR type field and an elastic K-field.

The domain dominated by the HRR type field will diminish as the material length scale l_1 increases. When the value of l_1/a is larger than 10^{-3}, the HRR type field seems to disappear.

Figures 5~7 show the distribution of stresses and strains ahead of the crack tip (at polar angle $\theta = 3.18°$). The parameters used here are: $\sigma_0/E = 0.2\%$, $\nu = 0.3$, $n = 0.2$, $K_I = 20\sigma_0(l_1)^{1/2}$, $l_{CS} = 2l_1$, $l_1/a = 10^{-3}$. The relation between l_{CS} and l_1 may be changed and this issue will be discussed later. The results for the classical deformation theory are also plotted in these figures for comparison.

Figure 5 shows the normalized stress components σ_{rr}/σ_0 and $\sigma_{\theta\theta}/\sigma_0$ versus the normalized distance to the crack tip r/l_1 ahead of the crack tip (at polar angle $\theta = 3.18°$). The normalized mean stress σ_m/σ_0 and normalized effective stress σ_e/σ_0 versus the normalized distance to the crack tip r/l_1 are plotted in Fig.6. The plastic zone size is a bit greater than $10l_1$, as seen from the domain where $\sigma_e/\sigma_0 \geq 1$ in Fig.6. It can be seen from these figures that the stress field at the outside domain tends to be the elastic K-field. Both the simplified strain gradient theory and the classical theory give the same straight line of slope $-1/2$ in this domain. There is usually a domain dominated by the HRR type field between the crack tip field dominated by the strain gradients and the outside elastic K-field. However, such a domain is found from Fig.5 and Fig.6 to be very small in comparison with some others' calculated results [17,23]. This is due to a relatively large value of l_1/a. Once the distance to the crack tip is less than $10l_1$, the stress level predicted by the simplified strain gradient theory increases much quicker than its counterpart in the classical theory. Therefore, it is obvious that the stress level near the crack tip in the simplified strain gradient theory is much higher than that in the classical deformation theory. In addition, it is shown in Fig.6 that near the crack tip the mean stress seems to have the square-root singularity while the singularity of the effective stress is slightly higher than the square-root singularity. Therefore the singularity of the stress components in Fig.5 is also slightly higher than the square-root one.

Figure 7 shows the hydrostatic strain ε_m and effective strain ε_e versus the normalized distance to the crack tip r/l_1 ahead of the crack tip (at polar angle $\theta = 3.18°$). It is found that ε_m is very close to ε_e and they both seem to have the square-root singularity. Since the stresses have the singularity slightly higher than the square-root one, we can see from Eq.(3.11)

that the strain energy w should have a singularity slightly higher than r^{-1}.

The physical background of the length scales is still uncertain now. Gao et al.[27] has given an expression which relates the length scales to some other material parameters, such as the Burger's vector, the shear modulus and the flow strength, but this expression still has to be verified. In most cases, it is supposed that a certain relation exists among the length scales, in order to reduce the number of independent parameters. Here we investigate a few cases: $l_{CS} = 0$, $l_{CS} = l_1$, $l_{CS} = 2l_1$ and $l_{CS} = 10l_1$, as shown in Fig.8. The other parameters are: $\sigma_0/E = 0.2\%$, $\nu = 0.3$, $n = 0.2$, $K_I = 20\sigma_0(l_1)^{1/2}$, $l_1/a = 10^{-3}$. It is seen that the larger the rotation gradient length scale l_{CS} is, the higher the stress level is. This means that in the present theory, the rotation gradients also have an important effect on the stress level besides the stretch gradients. This conclusion is different from that in a strain gradient theory with couple stress proposed by Chen and Wang[21]. In that theory, as long as the couple stresses keep being zero on all boundaries, they will be zero in the whole body and, as a result, the rotation gradients will have no effect at all. Furthermore, the near-tip slopes of the lines in Fig.8 are almost the same, therefore, the singularities in the four cases are the same. The domain dominated by the HRR type field is quite small. The larger l_{CS} is, the smaller the domain is.

The effect of the hardening exponent n on the stress field is shown in Fig.9. The cases of $n = 0.1$, 0.2, 0.3, 0.4 and 0.5 are calculated. The other parameters are: $\sigma_0/E = 0.2\%$, $\nu = 0.3$, $K_I = 20\sigma_0(l_1)^{1/2}$, $l_{CS} = 2l_1$, $l_1/a = 10^{-3}$. It is found that the greater n is, the greater the absolute value of the slope is, i.e., the greater the stress singularity is. In fact, it can be seen from Eq.(2.13) that the singularity of coefficient R is $r^{-1/2}$ and, as mentioned before, the singularity of the effective strain is also $r^{-1/2}$. Hence it can be concluded from Eq.(2.14) that the singularity of the effective stress is $r^{-(n+1)/2}$. In contrast, Jiang et al.[18] stated that the crack tip singularity in MSG plasticity is essentially independent of the plastic hardening exponent n. They attribute this to the fact that the density of geometrically necessary dislocations is much higher than that of statistically stored dislocations near a crack tip. In a similar way, we should say that according to our simplified strain gradient theory, statistically stored dislocations seem to play an important role as well as geometrically necessary dislocations near the crack tip. Again the domain

dominated by the HRR type field is small. The larger n is, the smaller the domain is.

The results under different load levels are shown in Fig.10. The parameters are: $\sigma_0/E = 0.2\%$, $\nu = 0.3$, $n = 0.2$, $l_{CS} = 2l_1$, $l_1/a = 10^{-3}$. The domain outside of the plastic zone is also the elastic K-field, as evidenced by the straight lines with the slope of $-1/2$ for larger r. At a smaller distance r to the crack tip, all curves approach to another set of straight lines, with the absolute value of the slope being slightly larger than $1/2$. This means that in our simplified strain gradient theory the singularity of stress near the crack tip is slightly higher than the square-root singularity in the elastic K-field. It is also observed from Fig.10 that the plastic zone size increases with the applied loading. Since the domain of the HRR type field is small, which is equivalent to say that the size of the domain dominated by the strain gradients increases with the applied loading.

The normalized J-integral $JE/[(1-\nu^2)K_I^2]$ versus the normalized distance to the crack tip r/l_1 ahead of the crack tip (at polar angle $\theta = 3.18°$) is shown in Fig.11. The material parameters are: $\sigma_0/E = 0.2\%$, $\nu = 0.3$, $n = 0.2$, $K_I = 20\sigma_0(l_1)^{1/2}$, $l_{CS} = 2l_1$, $l_1/a = 10^{-3}$. The calculated contour Γ is a circle centered at the crack tip. There are totally 100 such circles with different radii calculated here. It is observed from Fig.11 that the J-integral is path independent when the contour is in a remote domain ($r > 10l_1$). The domain in which the J-integral is path independent is consistent with the domain of the elastic K-field and the HRR type field, if there is any. However, in the domain dominated by the strain gradients (about $r \leq 10l_1$ in this case), the J-integral is no longer path independent. The J-integral increases monotonically as the radius r of the calculated circular contour Γ decreases. In fact, since the singularity of the energy density w is slightly larger than r^{-1}, the J-integral must monotonically increase as the radius r decreases.

The calculated results for Problem B are shown in Figs.12(a) and (b). Two cases are investigated: $l_1 = 1\,\mu m$ (Case I) and $l_1 = 0.1\,\mu m$ (Case II). The other parameters in both cases are: $\sigma_0/E = 0.2\%$, $\nu = 0.3$, $n = 0.2$, $\sigma_0 W/P = 500$, $l_{CS} = 2l_1$, $W = 10\,cm$. It can be seen from Fig.12 that in both cases the plastic zone size is about $2 \times 10^{-5}W$. Outside of the plastic zone, the material is linear-elastic, therefore the results in the simplified theory is almost identical with the classical results, represented by a straight line with the slope of $-1/2$. In fact, the re-

sults in Case I and Case II are also identical in the elastic zone. In both cases, as long as the material yields, the strain gradients make the stress level much higher than that in the classical deformation theory. No domain of the HRR type field is observed. The singularity of mean stress σ_m is almost the square-root singularity while the singularity of effective stress σ_e is higher than the square-root singularity. In the domain dominated by the strain gradients, the effective stress in Case I is much higher than its counterpart in Case II while the mean stress in Case I is only a little higher than that in Case II. Therefore, the change of l_1 seems to influence the effective stress more than it influences the mean stress. As the value of length scale l_1 increases, the effective stress increases remarkably while the mean stress increases only a little.
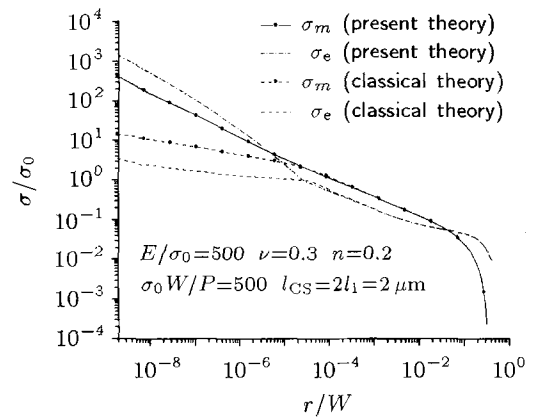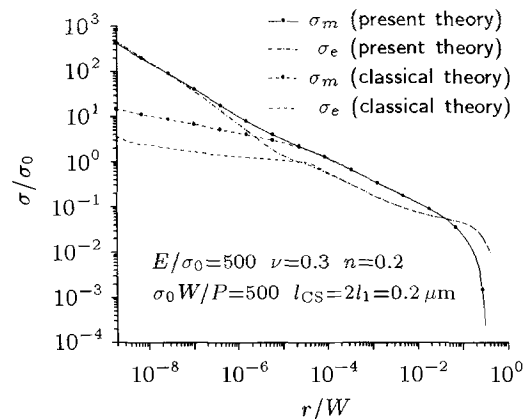

(a) $l_1 = 1\,\mu m$

(b) $l_1 = 0.1\,\mu m$

Fig.12 Normalized mean stress σ_m/σ_0 and effective stress σ_e/σ_0 versus normalized distance r/W in Problem B, for both the strain gradient theory and classical plasticity theory. $W = 10\,cm$

5 CONCLUSION

A simplified strain gradient theory is reviewed in this paper. The essential structure of the classical deformation theory is retained. No higher-order stresses are introduced into the simplified strain gradient theory. Strain gradient measures are incorporated as internal variables to increase the tangent modulus. In this way, the FEM formulation of the plane-strain mode-I cracks is developed. Two typical crack problems are studied, one is the crack tip field under the small scale yielding condition induced by a linear elastic mode-I K-field and the other is the complete field for a compact tension specimen. The numerical results show the elevation of the stress level, which may explain the experimental results of Elssner et al.[1]. It is observed that near the crack tip the singularity of the mean stress seems to be the square-root singularity while the singularity of the effective stress is slightly higher than the square-root singularity. Therefore the singularity of the stress components is also higher than the square-root singularity. In addition, both the hydrostatic strain and effective strain are of square-root singularity. As a result, the J-integral is path dependent in the domain dominated by the strain gradients. The hardening exponent n is found to have some effects on the singularity of stresses, while some other parameters, such as the length scales and the stress density factor, seem to have no such effects.

REFERENCES

1 Elssner G, Korn D, Ruehle M. The influence of interface impurities on fracture energy of UHV diffusion bonded metal-ceramic bicrystals. *Scripta Metall Mater*, 1994, 31: 1037

2 Hutchinson JW. Linking scales in mechanics. In: Karihaloo BL, Mai YW, Ripley MI, et al. eds. Advances in Fracture Research. New York: Pergamon Press, 1997. 1

3 Fleck NA, Hutchinson JW. A phenomenological theory for strain gradient effects in plasticity. *J Mech Phys Solids*, 1993, 41: 1825

4 Fleck NA, Muller GM, Ashby MF, et al. Strain gradient plasticity: theory and experiment. *Acta Metall Mater*, 1994, 42: 475

5 Huang Y, Zhang L, Guo TF, et al. Near-tip fields for cracks in materials with strain-gradient effects. In: Willis JR ed. Proceeding of IUTAM Symposium on Nonlinear Analysis of Fracture. Cambridge, England: Kluwer Academic Publishers, 1995. 231

6 Huang Y, Zhang L, Guo TF, et al. Mixed mode near-tip fields for cracks for cracks in materials with

strain-gradient effects. *J Mech Phys Solids*, 1997, 45: 439~465

7 Xia ZC, Hutchinson JW. Crack tip fields in strain gradient plasticity. *J Mech Phys Solids*, 1996, 44: 1621~1648

8 Chen JY, Huang Y, Hwang KC. Mode I and mode II plane-stress near-tip fields for cracks in materials with strain gradient effects. *Key Engng Mater*, 1998, 145: 19~28

9 Huang Y, Zhang L, Guo TF, et al. Fracture of materials with strain gradient effects. In: Karihaloo BL, Mai YW, Ripley MI, et al. eds. Advances in Fracture Research. Amsterdam: Pergamon Press, 1997. 2275~2286

10 Wei Y, Hutchinson JW. Steady-state crack growth and work of fracture for solids characterized by strain gradient plasticity. *J Mech Phys Solids*, 1997, 45: 1253~1273

11 Chen JY, Wei Y, Huang Y, et al. The crack tip fields in strain gradient plasticity: the asymptotic and numerical analyses. *Engng Fract Mech*, 1999, 64: 625~648

12 Shi MX., Huang Y, Hwang KC. Fracture in the higher-order elastic continuum. *J Mech Phys Solids*, 2000, 48: 2513~2538

13 Fleck NA, Hutchinson JW. Strain gradient plasticity. In: Hutchinson JW, Wu TY eds. Advances in Applied Mechanics, vol. 33. New York: Academic Press, 1997. 295

14 Gao H, Huang Y, Nix WD, et al. Mechanism-based strain gradient plasticity——I. Theory. *J Mech Phys Solids*, 1999, 47: 1239

15 Huang Y, Gao H, Nix WD, et al. Mechanism-based strain gradient plasticity——II. Analysis. *J Mech Phys Solids*, 2000, 48: 99

16 Shi MX, Huang Y, Gao H, et al. Non-existence of separable crack tip field in mechanism-based strain gradient plasticity. *Int J Solids Struct*, 2000, 37: 5995~6010

17 Jiang H, Huang Y, Zhuang Z, et al. Fracture in mechanism-based strain gradient plasticity. *J Mech Phys Solids*, 2001, 49: 979~993

18 Acharya A, Bassani JL. On non-local flow theories that preserve the classical structure of incremental boundary value problems. In: Pieau A, Zaoui A eds. IUTAM Symposium on Micromechanics of Plasticity and Damage of Multiphase Materials, Paris, 1995-8-29~9-1. Netherlands: Kluwer Academic Publisher, 1996. 3~9

19 Chen SH, Wang TC. A new hardening law for strain gradient plasticity. *Acta Mater*, 2000, 48: 3997~4005

20 Chen SH, Wang TC. A new deformation theory for strain gradient effects. *Int J Plasticity*, 2002, 18: 971~995

21 Chen SH, Wang TC. Strain gradient theory with couple stress for crystalline solids. *Eur J Mech A / Solids*, 2001, 20: 739~756

22 Chen SH, Wang TC. Mode I crack tip field with strain

gradient effects. *Acta Mechanica Solida Sinica*, 2000, 13(4): 290~298

23 Chen SH, Wang TC. Finite element solutions for plane-strain mode I crack with strain gradient effects. *Int J Solids Struct*, 2002, 39(5): 1241~1257

24 Ashby MF. The deformation of plastically non-homogeneous alloys. *Philosophical Magazine*, 1970, 21: 399

25 Smyshlyaev VP, Fleck NA. The role of strain gradients in the grain size effect for polycrystals. *J Mech Phys Solids*, 1996, 44: 465

26 Aifantis EC. On the microstructural origin of certain inelastic models. *Trans ASME J Engng Mater Tech*, 1984, 106: 326~330

27 Gao H, Huang Y, Nix WD. Modeling plasticity at the micrometer scale. *Naturewissenschaften*, 1999, 86: 507~515